Reducing Positioning Uncertainty of Objects by Robot Pushing

Zdravko Balorda and Tadej Bajd

Abstract—**Robotic applications often involve manipulation of objects where position and orientation are not perfectly known. Pushing an object for instance by a fence, can be employed to accurately align parts, reducing uncertainty to only one degree of freedom. In this paper a pushing task involving two fingers that completely constrains an object in a plane is proposed. The stability of orientation and position of an object being pushed is discussed. The solution obtained is unique despite the fact that the distribution of forces supporting the object cannot, in general, be known. The proposed task of pushing is simple although some preliminary information about the initial position and orientation of an object is required. An approach to avoid the ambiguity in orientation, owing to the effect of friction between the object and the pusher, by introducing up and down movement of the pusher is also presented.**

I. Introduction

A key problem in robot manipulation is the presence of uncertainty. Robots must operate in a real environment that is inherently uncertain. In most industrial applications objects are handled with the help of carefully designed mechanical fixtures that supply parts in predetermined orientation and position. In such applications it is usually assumed that there is no uncertainty left since the objects, tasks, environment, and motions are well known in advance. The cost of this approach can be very high: reducing the uncertainty inherent in a task itself is difficult, while it is impossible to eliminate it entirely [1]. Instead of trying to eliminate the uncertainty from manipulation tasks it is our goal to develop robot operations that can tolerate this uncertainty. An operation of this kind is a maneuver of pushing an object: it can, to a large extent, tolerate inaccuracy in orientation. A use of pushing in robot manipulation was demonstrated in the literature by a hinge-plate grasping operation described by Paul and Mason [2]. Beside providing grasping of a hinge-plate the pushing maneuver also eliminated initial variations in the position of a hinge-plate without requiring any sensory feedback. Fearing [3] examined robot grasping and developed an analysis of motion and stability of an object being squeezed by two point-fingers. His maneuver did not reduce entirely the uncertainty of the object position owing to the ambiguity of two-point grasp with friction. Trinkle [4] also discussed grasping in the presence of uncertainty by studying the mechanics of lifting a slippery two-dimensional object. Brost [1] presented an effective method for planning grasping operations in the presence of uncertainty. Three types of grasping operations were proposed that can successfully remove two degrees of uncertainty from the object position. These procedures require certain knowledge about the shape and approximate position and orientation of an object prior to manipulation. Another example of how to eliminate uncertainty was shown by Peshkin and Sanderson [5] who designed a part-feeder that can correctly orient parts with random initial orientations. A simple and effective technique that accurately orients parts of complex shape was presented by Grossman [6].

Manuscript received August 5, 1991; revised October 11, 1993. This work was supported by the Republic of Slovenia Ministry of Science and Technology.

The authors are with the University of Ljubljana, Faculty of Electrical and Computer Engineering, Laboratory for Robotics, 61000 Ljubljana, Trzaska 25, Slovenia.

IEEE Log Number 9402208.

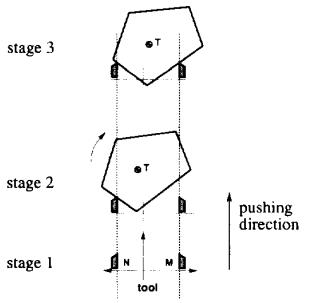

Fig. 1. Three stages of the operation of pushing.

The key issue in this paper is the improvement of accuracy of positioning an object in all degrees of freedom in a plane obtained by robot pushing. The early stage work on this subject is presented in [7].

Pushing an object is a complex mechanical process. Frictional forces play a dominant role and the forces applied are in general unpredictable. To understand this and similar operations, Mason [2] has theoretically described the conditions required for translation, clockwise (CW), and counterclockwise (CCW) rotation of a workpiece being pushed. The task proposed here involves a two-finger tool or a gripper attached to a robot end effector. The object is assumed to be a convex polygon, although this assumption can be relaxed. Assuming that position and orientation are approximately known prior to the operation, the initial position of the tool and the direction of movement can be chosen. As the tool advances it would strike the object (Fig. 1). If the robot trajectory is chosen correctly, the fingers will contact the object with its corner between them. It will be shown that in the absence of friction this configuration of contact points uniquely constrains the position of an object in all degrees of freedom. Nevertheless, there is an ambiguity in orientation of the object being pushed due to the friction at the points of contact with the pusher. This ambiguity was almost completely eliminated by introducing up and down movement of the pusher during the operation. However, complete description of the task rises a number of questions. What is the optimal finger spread? What is the best finger position? What is the range of lateral and orientation positioning uncertainty that can be tolerated? What is the pushing distance required? What are the conditions under which the operation is guaranteed to succeed? Some of the answers are presented in this paper, while for others complete solutions are not clear at the time.

II. Methods

Throughout the paper the following notation is used: $\mathcal{P}, \mathcal{G}$ denotes coordinate frames, M, N, C are points in a plane, ${}^{\mathcal{P}}\vec{M}$ is a vector describing point M with respect to $\mathcal{P}$, and $x_{\mathcal{P}}, y_{\mathcal{P}}$ are the x-, y-axis of the coordinate frame $\mathcal{P}$.

Let $\mathcal{P}$ be a polygonal part that is to be pushed into a desired position and orientation. Associated with the part is a coordinate system $\mathcal{P}$, where the $x_{\mathcal{P}}$-axis is aligned with an edge of the part and the origin is at the corner. The points of the object $\mathcal{P}$ are described with respect to this coordinate system (Fig. 2). Let ${}^{\mathcal{P}}\vec{T} = (\eta_T, \xi_T)^T$ be the vector describing the center of mass of the part with respect to $\mathcal{P}$ and α be the angle of the corner under consideration. Note that

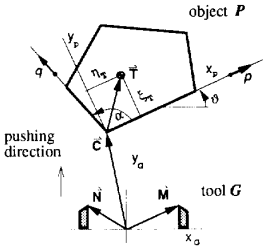

Fig. 2. Definitions of geometrical parameters.

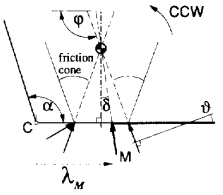

Fig. 3. Valid contact configurations at the right finger M.

there are many different objects, not necessarily polygonal, whose shape would fit the above description.

Let $\mathcal{G}$ be a two-finger tool attached to the robot end effector. Associated with the tool is a coordinate system $\mathcal{G}$ where the positions of contact points (fingers) are defined. There is no motion of the contact points relative to $\mathcal{G}$ during the operation. The coordinate system $\mathcal{G}$ is oriented in such a way that $y_{\mathcal{G}}$-axis points in the direction of motion while its origin is placed arbitrarily. It is considered useful to choose the position of the origin so that it coincides with the origin of the robot's last link. Let $\vec{M}$ and $\vec{N}$ be the vectors describing position of the left and right finger of the tool with respect to the coordinate system $\mathcal{G}$. Thus, the mathematical description of the problem must yield a system of equations describing the position of the center of mass of the object ${}^{\mathcal{G}}\vec{T}$ with respect to the origin of $\mathcal{G}$ and the angle ϑ between the edge of the object and the $x_{\mathcal{G}}$-axis of $\mathcal{G}$ (the orientation of the object).

To analyze the mechanics of the pushing operation it is necessary to prescribe conditions under which the operation takes place. The conditions are:

1) The object is considered to be a two dimensional rigid body with a finite mass. At least one convex vertex is necessary.
2) The friction is Coulomb dry friction. No velocity dependent forces are expected as occurring in viscous friction. The distribution of both, dynamic and static coefficient of surface friction μ_s must be
$$\mu_s(x, y) = const. \tag{1}$$
3) The supporting surface is assumed to be smooth and homogeneous. It follows that the center of friction [2], if it exists, coincides with the centroid of pressure distribution.
4) The support forces due to gravity are distributed over the entire contact area between the object and the supporting surface. The pressure distribution is unknown, yet all the supporting forces point in the same direction.
5) Motion is analyzed in terms of quasi-static mechanics. All forces/torques owing to moments of inertia are neglected. Movement velocities are small enough so that the energy accumulated is much smaller then the work needed to overcome the friction.
6) Contact between a body and fingers is considered to be a simple point contact. Fingers are modeled as a line normal to the supporting surface which forms point contact with a two dimensional body. In the beginning it will be assumed that the contact points are frictionless. Thus, the contact forces lie along contact normals. No tangential forces are possible. All torques around a contact point are equal to zero.

The progress of the pushing operation through different stages is shown in Fig. 1. Starting with no contact (stage 1), the tool proceeds in the direction shown by an arrow. When the first finger strikes the object, the object will start to rotate with respect to the contact point (stage 2). The object rotates and eventually the contact is made by the second finger at stage 3. During stage 3 the object will rotate further until a final orientation is reached. Afterwards, the object will purely translate along the direction of movement of the tool.

The goal of the approaching stage is to provide CW rotation if the finger N first strikes the object or CCW rotation for the finger M. According to Mason's pushing theory [8] it is sufficient if any two of three lines—the pushing line, and the left and right side of the friction cone—lies on the appropriate side of the center of mass: the left side produces a CW rotation and the right side produces a CCW rotation. Secondly, the direction of rotation must be preserved throughout stage 2. For sticking contact this condition is always satisfied. For sliding contact, violation of this condition depends on the direction of sliding. If the direction of sliding is toward the vertex C it is possible for the friction cone to pass the center of mass, thus reversing the direction of rotation. Assuming the direction of rotation is correct for the given finger, the direction of sliding must point away from the vertex (Fig. 3).

It follows, for the right finger M, both conditions are satisfied if the line of pushing always lies to the right of the center of mass and if it lies inside or to the right of the friction cone. The same rule can be applied to the left finger N if the term right is changed for left. To apply this rule two parameters need to be specified. These are the contact point along the facet and the pushing direction. For the right finger M (Fig. 3) the candidate contact points are denoted by a thick line and the candidate pushing directions lie inside the angle φ. Pushing directions are bounded by a direction along the facet and the left side of the friction cone. The left bound on the range of candidate contact points (λ_M) depends on pushing direction, however. In Fig. 3 for a given pushing direction shown by an arrow, all points to the right of the arrow are valid contact points.

The above rule is expressed in terms of an angle δ
$$\delta_M = \begin{cases} \vartheta & ; -\arctan(\mu_c) < \vartheta < \arctan(\mu_c), \\ \arctan(\mu_c) & ; \vartheta \geq \arctan(\mu_c) \end{cases} \tag{2}$$
within which the left bound in valid contact points changes. The term μ_c represents contact friction. The angle ϑ is the orientation of object as was defined previously (Fig. 2). Equation (2) corresponds to the finger M, the left bound λ_M being equal to
$$\lambda_M(\vartheta) = \eta_T - \xi_T \cdot \tan(\delta_M). \tag{3}$$
For the left finger N, the expressions (2) and (3) are as follows:
$$\delta_N = \begin{cases} \pi - \vartheta - \alpha & ; -\arctan(\mu_c) < \pi - \vartheta - \alpha < \arctan(\mu_c), \\ \arctan(\mu_c) & ; \pi - \vartheta - \alpha \geq \arctan(\mu_c) \end{cases} \tag{4}$$
$$\lambda_N(\vartheta) = \vec{T} \cdot (\vec{\alpha}) - \vec{T} \cdot (\alpha - \vec{\pi}/2) \tan(\delta_N) \tag{5}$$
where angle vector $(\vec{\alpha})$ designates a unit vector $(\cos\alpha, \sin\alpha)^T$.

From the above equations it is possible to calculate bounds on theposition of vertex C of object for a given orientation ϑ. Approaching the object in a way that vertex C lies inside these

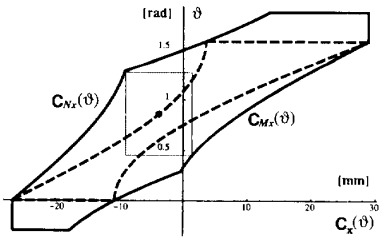

Fig. 4. The limits in lateral and orientation positioning error.

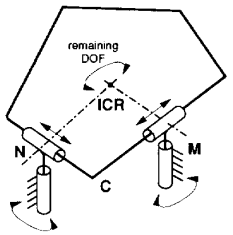

Fig. 5. A mechanism representing an object touching two-finger tool.

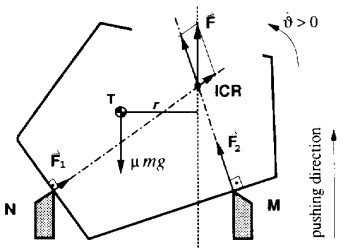

Fig. 6. Forces acting on the object being pushed.

bounds will produce valid contact configurations with either finger. Note that only x coordinate of $\vec{C}$ is important, as long as we make sure the object is in front of the tool (see also Fig. 1). The leftmost and rightmost position of vertex C are

$$C_{Nx}(\vartheta) = N_x - \lambda_N(\vartheta)\cos(\vartheta + \alpha),$$
$$C_{Mx}(\vartheta) = M_x - \lambda_M(\vartheta)\cos(\vartheta), \tag{6}$$

respectively. The range of available pushing directions in terms of object orientation is equal to

$$-\arctan(\mu_c) < \vartheta < \pi - \alpha + \arctan(\mu_c). \tag{7}$$

The expressions (6) and (7) form a bounded region in (C_x, ϑ) plane (Fig. 4) where all points inside this region correspond to a pushing operation producing correct motion of object during stage 2. The expressions for C_{Nx}, C_{Mx} in (6) need further modification, however. For instance, if $\vartheta > \pi/2$, the facet the finger M should contact, becomes unreachable. The same holds true for the left finger N if $\vartheta < \pi/2 - \alpha$. When either of these two conditions becomes true, it must be assured that the corresponding finger will at least miss the object to avoid pushing at the same facet by both fingers. The rightmost limit in vertex position is then equal to M_x and the leftmost to N_x. In Fig. 4 the vertical segment in $C_{Nx}(\vartheta)$ and $C_{Mx}(\vartheta)$ represents this case. The region in Fig. 4 outlined by a dashed line corresponds to frictionless fingers, while a continuous line bounds the region corresponding to $\mu_c = 0.3$. The description of the object and the tool is taken from the example shown at the end of the paper (Table I, middle row). The contact friction was chosen freely to demonstrate its effect on the ability of operation to handle uncertainty. Clearly, the friction at fingers helps: the region becomes larger if the friction exists. Also, spreading the fingers has the similar effect. A wider tool can handle greater uncertainty than a narrower one. This discussion implies that the facet length is infinite, however. Spreading the fingers will ultimately cause the object to slip through the fingers. The recommended distance between the fingers is the least one of all the distances obtained from calculating the cross-sections of an object in the range of orientations given by expression (7).

Let the errors in position and orientation be $\varepsilon_x, \varepsilon_\vartheta$, respectively. In (C_x, ϑ) plane a pair $(\varepsilon_x, \varepsilon_\vartheta)$ represents a rectangular area where a point inside this area indicates possible position and orientation. Let the center point of the rectangle be the nominal position and orientation with respect to the fingers. By changing pushing direction and starting point this position and orientation also change. Hence, the rectangle can be placed arbitrarily in the plane (C_x, ϑ) by choosing a different pushing operation. The pushing operation that can handle the uncertainty given by the worst case limits in error $(\varepsilon_x, \varepsilon_\vartheta)$ is the one that places the rectangle inside the bounded region as is shown in Fig. 4. The center point designates the pushing operation guaranteeing that during stage 2 the object will move toward the other finger reaching stage 3 at some point. Finding the best possible operation is a problem of task planning. The early work on this subject is presented in [9].

To understand the situation during the stage 3, one must consider the constraints imposed upon the object, and the forces acting on it.

A rigid body touching a tool at two points can be represented by a simple mechanism whose mobility is easier to explore (Fig. 5). The points of contact, namely M and N, have each two degrees of freedom: one translation along the edge of the object, and one rotation around contact point.

Altogether there are four DOF's. Taking into account also one closed kinematic chain, the mobility is calculated by the Grübler's formula:

$$\mathcal{M} = \sum_{i=1}^{n} f_i - 3l = 4 - 3 = 1 \tag{8}$$

where i is a joint index, f_i is the number of DOF's for the joint i and l is the number of closed kinematic chains. The total mobility $\mathcal{M}$ equals to 1, and corresponds to a rotation around the intersecting point of the two lines along the contact normals (dashed lines, Fig. 5). At any arbitrary orientation angle ϑ this point is elsewhere in a plane, so it is an *instantaneous center of rotation* (ICR) and the mechanism is called a *transitory substitute-mechanism* [10].

Supposing the movement of a body is a pure translation, the center of friction exists [2], and according to the assumptions about friction it coincides with the center of mass. Frictional force due to support friction $\mu_s mg$ is drawn in the opposite direction with respect to the motion velocity (Fig. 6). Taking into account an equal force $\vec{F}$ in the opposite direction and dividing it into two components along the contact normals at points M, N, the contact forces $\vec{F}_1, \vec{F}_2$ (Fig. 6) are obtained.

The position of the ICR becomes known by constructing the lines along both contact normals, so the torques acting on the object can be determined. Contact forces $\vec{F}_1$ and $\vec{F}_2$ do not induce any torques around ICR because they are acting along the contact normals: their levers are equal to zero. The only torque induced is by the support friction force

$$|\vec{M}_f| = \mu_s mg \cdot r. \tag{9}$$

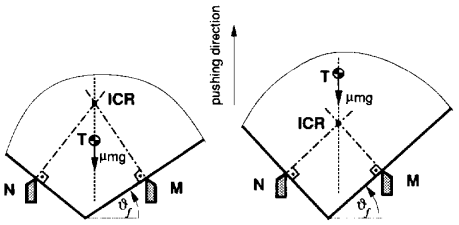

Fig. 7. The final orientation for two different objects.

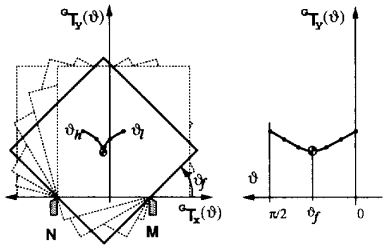

Fig. 8. The plot of the tip of (a) ${}^{\mathcal{G}}\vec{T}$. (b) ${}^{\mathcal{G}}T_y(\vartheta)$.

To maintain pure translation an equal torque must be induced around ICR in the opposite direction. The only way to induce such a torque is by tangential forces at contact points M, N. As these are frictionless contacts it follows that the object will rotate in a counterclockwise direction. The final orientation is achieved when $|\vec{M}_f| = 0$. From (9) it follows that r must be equal to zero. Therefore, the center of friction (also the center of mass) must lie somewhere on the line along the direction of pushing through the ICR (Fig. 7). Note that only the sense of rotation can be described in this way. During rotation of the body, the friction force cannot be defined easily due to unavailability of the center of friction: the function of pressure distribution has to be known to fully describe the friction force. However, the conclusion about the final orientation holds true.

Note also, the analogous behaviour of an object being hung in a vertical plane between two horizontal frictionless bars. The body rotates due to gravity and reaches the static equilibrium in exactly the same orientation as above. It is the orientation satisfying the minimum of potential energy. Though it seems obvious that minimizing the potential energy would give stable orientation of the object also for pushing operation, one should consider the nature of frictional forces being a non-conservative system. Only in a special case when a pure translation occurs this analogy can be observed.

Consequently, the criterion of minimal "potential energy" can be applied: a body is expected to slip between the fingers as deep as possible. This result needs further elaboration, however. As will be discussed later, to determine the sense of rotation and whether the object will stay in contact with both fingers during stage 3, it is not always enough to consider the position of the center of mass with respect to ICR, only.

A. Estimating Final Orientation

An object in contact with both fingers represents a closed planar kinematic chain with one degree of freedom, namely rotation. Such a system is fully described by a function of one variable. Final orientation is defined in the local coordinate system of the tool independently of the actual world coordinates. The transformation between the two coordinate systems is trivial and will not be considered here.

The position and orientation of the object are described by two lines coinciding with the two edges of the object. According to the adopted description of an object we are not concerned about the rest of the part as long as the coordinates of the point $\vec{T}$ are known.

The solution to kinematics of the mechanism (Fig. 5) in terms of thevertex position $\vec{C} = (C_x, C_y)^T$ after rearranging yields:

$$C_x(\vartheta) = [(M_y - N_y)\cos\vartheta - (M_x - N_x)\sin\vartheta]\frac{\cos(\vartheta+\alpha)}{\sin\alpha} + N_x \tag{10}$$

$$C_y(\vartheta) = [(M_y - N_y)\cos\vartheta - (M_x - N_x)\sin\vartheta]\frac{\sin(\vartheta+\alpha)}{\sin\alpha} + N_y. \tag{11}$$

The position of the center of mass $\vec{T}$ with respect to $\mathcal{G}$ [11] equals:

$${}^{\mathcal{G}}\vec{T} = \left[\mathrm{Trans}(\vec{C})\cdot\mathrm{Rot}(\vec{k},\vartheta)\right]\cdot\vec{T} \tag{12}$$

where $\vec{k}$ is the Cartesian unit vector along the z-axis.

Equation (12) specifies the position of the center of mass of the part for any angle ϑ and any known position of the fingers. The stable position required is derived by minimizing the y coordinate of the ${}^{\mathcal{G}}\vec{T}$

$${}^{\mathcal{G}}T_y(\vartheta) = \eta_T\sin\vartheta + \xi_T\cos\vartheta + C_y(\vartheta). \tag{13}$$

Finding an angle ϑ, where (13) has a minimum, gives the solution to final orientation. The vector function (12) describes the path of the center of mass when the body is rotated while maintaining contact at both points M, N. To find the minimum, a domain of (12) and (13) with respect to the parameter ϑ has to be defined. Outside this domain the body is in contact with at most one of the two fingers. The plot of the function ${}^{\mathcal{G}}\vec{T}$ is shown in Fig. 8(a). For each particular orientation angle ϑ the corresponding position of the center of mass is marked by a dot. The plot begins at $\vartheta = 0$. Following the graph from the right to the left each subsequent dot represents the corresponding position of the center of mass when the object is rotated for additional 15° angle. In the case shown the plot ends at $\vartheta = \pi/2$.

Let the starting orientation of the body at the beginning of the plot be ϑ_l and the one at the end be ϑ_h. The range of angles $\vartheta \in (\vartheta_l, \vartheta_h)$ defines the domain of the function (12). The endpoints are, generally, expressed as

$$\vartheta_l = \max\begin{cases}\arctan[(M_y - N_y)/(M_x - N_x)]\\ \pi/2 - \alpha\\ 0\end{cases} \tag{14}$$

$$\vartheta_h = \min\begin{cases}\pi - \alpha + \arctan[(M_y - N_y)/(M_x - N_x)]\\ \pi - \alpha\\ \pi/2\end{cases}. \tag{15}$$

The endpoints ϑ_l, ϑ_h are obtained by testing all possible orientations of the object by taking into account the fact that contact normals cannot have any component opposite to the direction of pushing. The first row in (14) and (15) defines the limits when either facet is aligned with the line joining the fingers, while the last two rows assert that the components of the contact normals perpendicular to the line of pushing oppose one another, which is a necessary condition for attaining a stable equilibrium.

The y coordinate of ${}^{\mathcal{G}}\vec{T}$ (12) with respect to orientation angle ϑ is presented in (Fig. 8(b)) The function ${}^{\mathcal{G}}T_y(\vartheta)$ (13) has unique local minimum. It can be shown that at most one minimum could occur over the interval $(0, \pi/2)$ along ϑ-axis, hence the interval $(\vartheta_l, \vartheta_h)$ being always a subset of $(0, \pi/2)$ cannot embrace more then a single minimum, if any.

By solving for ϑ_f where function (13) has a minimum, also the position of the object with respect to the tool is known. A Brent's

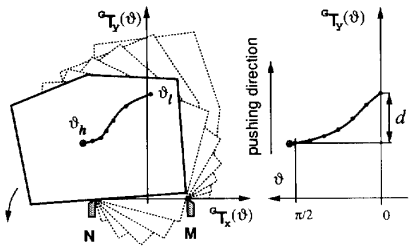

Fig. 9. The case leading to a task failure.

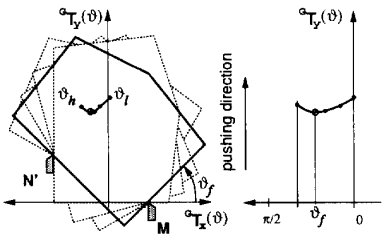

Fig. 10. Improved stability by a proper configuration of the tool.

minimization method [12] was applied to solve for ϑ_f. It converges very quickly, because the minimum behaves parabolically.

B. Task Failure

Pushing by a single point can only constrain the object in the direction against the contact normal. Only in a special case, when pushing a concave object, it may improve the positioning accuracy. In the previous section it has been shown that pushing with two point-contacts leads to a stable orientation in a wider class of objects. Note that the position of the object is also known if the contact normals are not parallel: the normals are parallel when both fingers are pushing at the same edge (equivalent to pushing by a fence).

However, in certain cases the two-point pushing operation may fail.An example is when both fingers are closely together. In the limiting case, when $\vec{M} = \vec{N}$ the task becomes single point pushing operation. Another case when the task is likely to fail is shown in Fig. 9 where the ${}^{\mathcal{G}}\vec{T}(\vartheta)$ and its y coordinate ${}^{\mathcal{G}}T_y(\vartheta)$ are presented. The plots are obtained in the same way as those in Fig. 8 but for a different object. The plots correspond to fingers at positions M and N. In that case (fingers at M, N), the curve ${}^{\mathcal{G}}T_y(\vartheta)$ is monotonic and does not have a minimum at all. The object will rotate during pushing in CCW direction, for any given initial orientation between $(0, \pi/2)$. The object may reach the final orientation which is at $\pi/2$ but the contact at finger M will be lost under the slightest perturbation in CCW direction. Further advancing of the tool will push the object away to the left, instead of catching it between the fingers. The final rest orientation in this case cannot be referred to as a stable one. The final orientation is considered stable if the object tends to rotate back to the same orientation after being perturbed in any direction during pushing. The above instability can also be observed with an object being hung in a vertical plane: the object will always fall off to the left of the supporting bars regardless the initial orientation. Making the tool wider might be considered to be a solution but, ultimately it is an ineffective one, because the object would slip between the fingers if the tool is too wide. A more appropriate solution is shown in Fig. 10, where the fingers are at positions M, N'.

An important aspect is the symmetry of the object. Here, the symmetry of the corner with respect to the mass distribution is considered. The object in Fig. 8 whose center of mass lies on the line bisecting the corner is characterized by this symmetry. The stability of the final orientation is such that it can resist equally to perturbation in any direction during pushing. The plot of ${}^{\mathcal{G}}T_y(\vartheta)$ is also symmetric. As a measure for this symmetry we adopted the distance d (Fig. 9) between both ends ϑ_l, ϑ_h of the ${}^{\mathcal{G}}T_y(\vartheta)$. For a symmetric object the distance d can be set to zero as in Fig. 8 by aligning both fingers $(M_y = N_y = 0)$. In the gravitational field this would provide that the same potential energy change is needed to perturb the object in either direction. At the same time the largest resistance to perturbations in orientation is provided. Thus, the stability in final rest orientation of object can be improved by applying the following criterion function:

$$|{}^{\mathcal{G}}T_y(\vartheta_h) - {}^{\mathcal{G}}T_y(\vartheta_l)| = d = \min \tag{16}$$

which results in a configuration of fingers that minimizes the distance d.

Intuitively, we conclude that there are only two dimensions in ${}^{\mathcal{G}}T_y(\vartheta)$ (13), namely $(M_x - N_x)$ and $(M_y - N_y)$. The shape of the graph (Fig. 10) depends only on the width $(M_x - N_x)$ and the height $(M_y - N_y)$ of the tool. Note that the terms width and height are defined with respect to the pushing direction. In our case the tool was only able to rotate around the z-axis. The distance between the fingers was fixed, hence rotating the tool while preserving the pushing direction increased the height at the expense of the width. An angle γ was introduced for which the tool was rotated before the operation. In the experiments presented in Figs. 13 and 14 the tool was rotated for such an angle γ by applying the criterion (16). As may intuitively be expected, the finger that is closer to the center of mass is positioned slightly forward giving improved "support" to the object during pushing.

To conclude, the width of the tool should be chosen as large as possible, depending on the overall dimensions of the object, while the optimal height is found by applying the criterion (16).

The discussion presented here is applicable to a certain class of objects. This class of objects is characterized by the position of the center of mass which must lie between the ICR and the fingers: it is the area of intersection of the inner halfplanes defined by the lines along the contact normals (a shaded region in Fig. 11). For this class of objects the discussion regarding the sense of rotation is correct. Also, during stage 3 the fingers would push the object toward one another holding the object safely in between. Hence, the result regarding the final rest orientation and the object stability holds true, too. However, it was observed through examples that the pushing operation can be applied to even wider class of objects, but it cannot be guaranteed to succeed. If the center of mass is outside the intersection area, both fingers may push the object in the same direction or away from one another. This does not immediately imply the task will fail, but rather that it may fail. What are the exact limits up to which the pushing operation is guaranteed to succeed remains an open issue.

C. Contact with Friction

Estimation of the results above is valid for frictionless contact points M, N. In reality one cannot rely on such an assumption. Fig. 11 shows the forces acting on an object when $\mu_c > 0$. The friction cones [2] are drawn around the contact normals.

Suppose the orientation of the body is far from its final orientation ϑ_f obtained if the contacts were frictionless. The center of mass is to the right of the ICR, causing a clockwise rotation during pushing. Thus, the contact forces act along the right side of the friction cones.

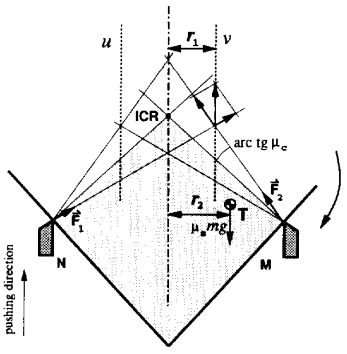

Fig. 11. The forces acting on the object during pushing by non-frictionless fingers.

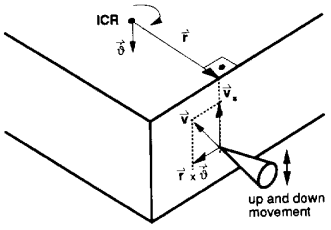

Fig. 12. The forces at the contact point with friction.

The static equilibrium ($\dot{\vartheta} = 0$) of the torques is reached as soon as the center of mass T crosses the line v, the distances being

$$r_1 = r_2. \tag{17}$$

Actually, the equilibrium may be reached at any orientation ϑ for which the center of mass lies between the lines u, v because the contact forces can be anywhere within the friction cone, yet satisfying (17).

Evidently, this would occur at some other angle ϑ then ϑ_f for which $r_1 = r_2 = r = 0$ (Figs. 6 and 7). The final rest angle ϑ_f would be no longer unique and the operation would express certain ambiguity in orientation.

The method proposed to reduce this effect of friction at contact points M, N is shown in Fig. 12. The tool is allowed to move up and down. As friction forces act in a direction opposite to a relative velocity at a contact point, the sum vector of the velocity in z direction (tool movement) and the velocity of the body ($\vec{r} \times \vec{\vartheta}$) is drawn.

In static equilibrium the tangential force at the contact point has only a vertical (z) component: tangential forces in the plane of consideration become zero when the object stops rotating because $\vec{r} \times \dot{\vartheta} = 0$. Thus, the contact friction at the final rest orientation cannot sustain any tangential force. This is exactly the case as though the fingers were frictionless: it can only occur at an angle ϑ that satisfies $r_1 = r_2 = 0$, which is the same condition for the final orientation as in the case of frictionless contact.

The effect of friction is eliminated simply by wiggling the fingers perpendicular to the surface during pushing. Such a motion can be performed by a robot selecting an appropriate motion trajectory or even better, by a vibrating device attached between the robot arm and the pushing tool. Notice however, that the pushing force will violate the assumption regarding the center of friction coinciding with the center of mass. While the forces along contact normals move the center of friction straight ahead in the pushing direction introducing no error in ϑ_f, it is not the case with the forces owing to wiggling the fingers. These forces are parallel with the gravitational force. During the upward tool motion the center of friction is shifted forward but also to the left or right, while during the downward motion the center of friction is shifted in the opposite direction. As a consequence the object will alternately rotate in a CW-CCW direction about ϑ_f introducing an error in orientation. This error is expected to be much smaller then the one introduced by friction at fingers as was also confirmed by experiments. One way to still reduce this error is by dynamically diminishing the shifting effect using a high speed vibrating device as proposed above. There is a design requirement that should be met when installing a vibrating device: the oscillating motion of the device must be purely vertical or else the object may repetitively be bounced of the fingers during pushing. This dynamic force would shift the center of friction in an undetermined way introducing an unknown error in the final rest orientation.

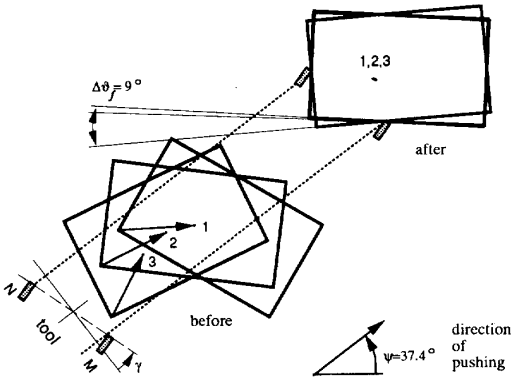

Fig. 13. Simple pushing operation.

III. Results

The method proposed was tested with different real objects. The tool used consisted of two prismatic bars, vertically mounted at the end effector of a robot SEIKO RT-2000. The robot has four degrees of freedom and cylindrically shaped working space. The objects were polygons with corner angles $\alpha = 60°, 90°, 120°$. To change the position of the center of mass three holes were drilled allowing insertion of different weights. The tool and the objects were made of Plexiglas. The supporting surface was covered with a paper. Two examples of pushing operation are shown in Figs. 13 and 14. The initial position of the tool is drawn and the direction of pushing is marked by an arrow. Fig. 13 shows an example of simple pushing operation without wiggling the tool up and down. The pushing direction ψ was chosen, considering the desired orientation of the object after completion of the pushing operation, using the formula

$$\psi = \omega - \vartheta_f + \pi/2,$$

where ω is the desired angle of orientation: in the examples presented the angle $\omega = 0$. The pushing distance of 150 mm was determined experimentally. The same operation of pushing was repeated three times: each time the initial position of object was different and the position and orientation, after the operation was completed, were marked by a line along the edge. The initial positions are marked by numbers 1,2,3 and the corresponding orientations with respect to the tool were $20°, 44°$ and $81°$, respectively. After the pushing operation was finished the final orientation was still uncertain because of the friction at the points of contact. The measured orientation difference $\Delta\vartheta_f$ was $9°$.

Fig. 14 shows the results of the pushing operation when the effect of friction was minimized by introducing the up and down movement of the tool. Again, the pushing operation was tested on three rather

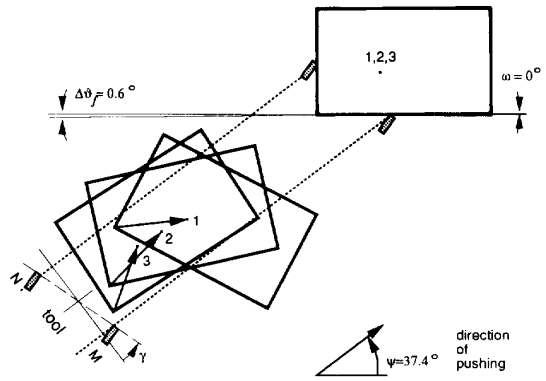

Fig. 14. Improving positioning accuracy by pushing with wiggling.

TABLE I
THE RESULTS OF THE EXPERIMENTS

Vertex angle	Center of mass [mm]		Mean value	Repeatability	$\vec{N}=\{-28.5,-2.5\}^T$ $\vec{M}=\{29.4,-2.5\}^T$ at $\gamma=0$
α	η_T	ξ_T	ω	$\Delta\omega$	γ
60°	71.8	43.8	0.4°	0.4°	-2.34°
	63.9	30.1	-0.5°	0.2°	5.73°
	86.2	30.2	-1°	1.5°	17.3°
90°	39.4	44.7	1.6°	0.5°	-7.5°
	39.6	30.2	0.2°	0.6°	14.8°
	60.8	30.4	-0.4°	0.9°	37.9°
120°	16.0	59.2	-1.4°	1.3°	0.8°
	0.2	59.1	0.3°	0.9°	-6.3°
	11.7	39.9	-2.5°	1°	-0.1°

random initial positions (1,2,3) and orientations (23°, 67°, and 87°, respectively). The final orientations obtained after the completion of pushing operations were more accurate then those from Fig. 13. This time the difference in orientations $\Delta\vartheta_f$ was 0.6°, only.

The results of pushing operations performed on other objects are presented in Table I.

The object being pushed is characterized by the vertex angle α and by the coordinates of the center of mass. A 50 g weight was inserted into different holes resulting in the change of the coordinates of the center of mass η_T, ξ_T. The fourth and the fifth column show the mean value of the orientation obtained and the absolute dispersion observed after three trials. The last column indicates the angle of rotation of the fingers before the operation. The second row at the 90° vertex angle applies to Fig. 14. The improved repeatability can be observed for objects whose center of mass is closer to the vertex and for those whose vertex angle is sharp. It may be that the effect of shifting the center of friction by vertical wiggling the fingers was the main source of dispersion of the results. The error in the desired value ω occurred probably owing to the inaccuracies in models of the objects and because of violating the assumptions to some extent.

IV. CONCLUSION

Application of pushing with single point pusher was in details discussed by Mason [8]. Here, we propose accurate orienting and positioning of a part to be performed by a robot-pushing operation which employs a two-finger gripper or a special tool. The fingers are used to push an object along a straight line. After the pushing maneuver is completed, the object can be grasped by reorienting the gripper and closing the fingers. The error evaluated in terms of part entropy [13] showed significant improvement of positioning accuracy—as much as 20 bits. The effect of the friction at the contact points was greatly reduced by wiggling the fingers perpendicular to the surface. The operation is extremely simple and improves the positioning capability of previously-reported operations. But, there are questions about the nature of this operation that have not yet been answered. The discussion presented remains to be extended to a wider class of objects. Nonetheless, the pushing operation proposed may be of practical importance in a number of robot applications.

The task can be implemented for various shapes and sizes of a workpiece. Economical justification of the task can be estimated by considering the cost of the operation due to slowing down of the robot performance as compared to the cost of sensors required for the same reduction in part entropy. In applications such as grasping a glass, accurate positioning of a glass is most effectively performed by the pushing operation proposed. The task of aligning a block in a corner, where there may be no room for the fingers, may successfully be performed only by using this pushing operation as a manipulating maneuver.

Further investigation is required, both theoretical and applied, to improve the approach described. The non-trivial problem of estimation of the pushing distance has to be solved. The worst case pushing distance can be estimated by extending the discussion in [14] where Peshkin presented a method based on a minimum power principle. However, the result would be valid only if the frictional forces at the fingers are neglected: the up and down wiggling of the tool introduces a viscous-like friction that may violate the minimum power principle, the pushing force being dependent on the angular velocity of the object.

Beside the problem of improving the positioning accuracy of an object, manipulating the object by a non-straight line pushing seems interesting. In a real application the working area available for the operation of pushing might be limited, so the trajectories of the tool must be planned considering other parameters in addition to the shape of the object.

REFERENCES

[1] R. C. Brost, "Automatic grasp planning in the presence of uncertainty," *Int. J. Robotics Res.*, vol. 7, no. 1, pp. 3–16, 1988.
[2] J. K. Salisbury and M. T. Mason, *Robot Hands and Mechanics of Manipulation*. Cambridge, MA: MIT Press, 1985.
[3] R. S. Fearing, "Simplified grasping and manipulation with dextrous robot hands," *IEEE J. Robotics Autom.*, vol. 2, pp. 188–195, 1986.
[4] J. C. Trinkle, "Grasp acquisition using liftability regions," in *Proc. IEEE Int. Conf. Robotics*, Philadelphia, PA, April 1988, pp. 88–92.
[5] M. A. Peshkin and A. C. Sanderson, "Planning robotic manipulation strategies for workpieces that slide,"*IEEE J.Robotics Autom.*, vol. 5, pp. 524–531, 1988.
[6] D. D. Grossman and M. W. Blasgen, "Orienting mechanical parts by computer controlled manipulator," *IEEE Trans. Syst. Man Cyber.*, vol. 5, pp. 561–565, 1975.
[7] Z. Balorda, "Reducing uncertainty of objects by robot pushing," in *Proc. IEEE Conf. Robotics Autom.*, Cincinnati, OH, 1990, pp. 1051–1056.
[8] M. T. Mason, "Mechanics and planning of manipulator pushing operations," *Int. J. Robotics Res.*, vol. 5, no. 3, pp. 53–71, 1986.
[9] Z. Balorda, "Automatic planning of robot pushing operations," in *Proc. IEEE Conf. Robotics Autom.*, Atlanta, GA, 1993, pp. 732–737.
[10] K. H. Hunt, *Kinematic Geometry of Mechanisms*. Oxford, U.K.: Oxford Univ. Press, 1978.
[11] R. P. Paul, *Robot Manipulators: Mathematics, Programming and Control*. Cambridge, MA: MIT Press, 1981.
[12] H. W. Press, P. B. Flannery, A. S. Teukolsky, and T. W. Vetterling, *Numerical Recipes—The Art of Scientific Computing*. Cambridge, U.K.: Cambridge University Press, 1986
[13] A. C. Sanderson, "Parts entropy methods for robotic assembly system design," in *Proc. IEEE Int. Conf. Robotics*, 1984.
[14] M. A. Peshkin,*Robotic Manipulation Strategies*. Englewood Cliffs, NJ: Prentice-Hall, 1990.